

1 *Supporting information for*

2 **Refining aerosol optical depth retrievals over land by constructing the**  
3 **relationship of spectral surface reflectances through deep learning: application**  
4 **to Himawari-8**

5  
6 Tianning Su<sup>1</sup>, Istvan Laszlo<sup>2,1</sup>, Zhanqing Li<sup>1</sup>, Jing Wei<sup>1</sup>, Satya Kalluri<sup>2</sup>

7  
8 <sup>1</sup>Department of Atmospheric and Oceanic Science & ESSIC, University of Maryland,

9 College Park, Maryland 20740, USA

10 <sup>2</sup>Center for Satellite Applications and Research, NOAA/NESDIS,

11 College Park, Maryland 20740, USA

12

13

14

15

16

17

18

19

20

21

22

23 **Table S1.** Spectral and spatial characteristics of different channels of the AHI sensor

<b>Channel ID</b>	<b>Wavelength</b>	<b>Spatial resolution</b>	<b>Channel ID</b>	<b>Wavelength</b>	<b>Spatial resolution</b>
1	0.47 $\mu\text{m}$	1 km	9	6.9 $\mu\text{m}$	2 km
2	0.51 $\mu\text{m}$	1 km	10	7.3 $\mu\text{m}$	2 km
3	0.64 $\mu\text{m}$	0.5 km	11	8.6 $\mu\text{m}$	2 km
4	0.86 $\mu\text{m}$	1 km	12	9.6 $\mu\text{m}$	2 km
5	1.61 $\mu\text{m}$	2 km	13	10.4 $\mu\text{m}$	2 km
6	2.25 $\mu\text{m}$	2 km	14	11.2 $\mu\text{m}$	2 km
7	3.9 $\mu\text{m}$	2 km	15	12.4 $\mu\text{m}$	2 km
8	6.2 $\mu\text{m}$	2km	16	13.3 $\mu\text{m}$	2km

24

**Table S2.** Microphysical properties of aerosol models used in the algorithm.

Aerosol Model	Mode	Volume median radius $r_v$	Standard Deviation $\sigma$	Volume Concentration $C_v$ ( $\mu\text{m}^3/\mu\text{m}^2$ )	Complex Refractive Index
Generic	Fine	$0.145 + 0.0203\tau^{\&}$	$0.3738 + 0.1365\tau$	$0.1642\tau^{0.7747}$	$1.43 - (0.008 - 0.002\tau)i$
	Coarse	$3.1007 + 0.3364\tau$	$0.7292 + 0.098\tau$	$0.1482\tau^{0.6846}$	
Urban	Fine	$0.1604 + 0.434\tau$	$0.3642 + 0.1529\tau$	$0.1718\tau^{0.8213}$	$1.42 - (0.007 - 0.0015\tau)i$
	Coarse	$3.3252 + 0.1411\tau$	$0.7595 + 0.1638\tau$	$0.0934\tau^{0.6394}$	
Smoke	Fine	$0.1335 + 0.0096\tau$	$0.3834 + 0.0794\tau$	$0.1748\tau^{0.8914}$	$1.51 - 0.02i$
	Coarse	$3.4479 + 0.9489\tau$	$0.7433 + 0.0409\tau$	$0.1043\tau^{0.6824}$	
Dust	Fine	$0.1416\tau^{-0.0519}$	$0.7561\tau^{0.148}$	$0.087\tau^{1.026}$	$(1.48\tau^{-0.021}) - (0.0025\tau^{0.132})i$ at $0.47\mu\text{m}^*$
	Coarse	2.20	$0.554\tau^{-0.0519}$	$0.6786\tau^{1.0569}$	$(1.48\tau^{-0.021}) - 0.002i$ at $0.55\mu\text{m}$ $(1.48\tau^{-0.021}) - (0.0018\tau^{-0.08})i$ at $0.66\mu\text{m}$ $(1.46\tau^{-0.040}) - (0.0018\tau^{-0.30})i$ at $2.12\mu\text{m}$

& AOD ( $\tau$ ) is the spectral value at  $0.55\mu\text{m}$ . The properties ( $r_v$ ,  $\sigma$ , and  $C_v$ ) of smoke and generic aerosol model are defined for  $\tau < 2.0$ , and  $\tau = 2.0$  is used in calculation when  $\tau > 2.0$ . Likewise, parameters of urban and dust aerosol are defined for  $\tau < 1.0$ , and  $\tau = 1.0$  is applied for higher  $\tau$ .

\* Refractive index at other shortwave wavelength is estimated by spectral interpolation/extrapolation.

**Table S3.** Criteria used for assigning retrieval quality over land.

Quality flag	Criteria
No Retrieval	1) Cloudy: input cloud mask is cloudy and any internal cloud, cirrus or inhomogeneity test fails; 2) Ephemeral water (from internal test).
Excluded  Low	1) Out of AOD range (-0.05, 5.0); 2) Solar zenith angle > 80°; 3) Satellite zenith angle > 60°; 4) Failed internal cloud reflectance test, but external cloud mask is clear or probably clear; 5) Failed internal cirrus test, but external cloud mask is clear or probably clear; 6) External cloud mask is cloudy or probably cloudy, but pass internal tests, and not heavy aerosol; 7) Coastal area (from external coastal mask); 8) Extrapolation to positive AOD is involved; 9) Retrieval residual > 0.5; 10) $\sigma_{0.47}^{2 \times 2} > 0.008$ with 1-km 0.47- $\mu\text{m}$ reflectances or $\sigma_{0.47}^{3 \times 3} > 0.012$ with 2-km 0.47- $\mu\text{m}$ reflectances.
Used  Medium	1) Adjacent to cloudy pixel; 2) $\sigma_{0.47}^{2 \times 2} > 0.004$ with 1-km 0.47- $\mu\text{m}$ reflectances or $\sigma_{0.47}^{3 \times 3} > 0.006$ with 2-km 0.47- $\mu\text{m}$ reflectances; 3) Retrieval residual > 0.4; 4) External cloud mask is ‘probably clear’.
High	Remaining retrievals

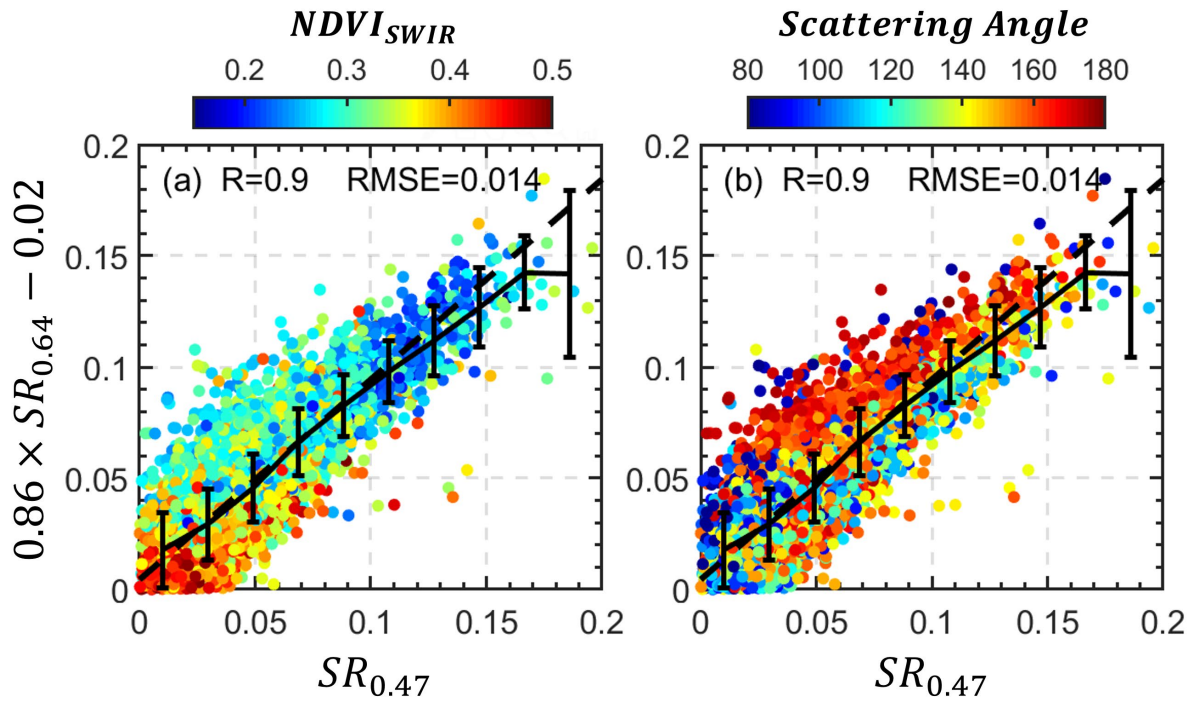


**Fig. S1.** The comparison between “true”  $SR_{0.47}$  and  $SR_{0.47}$  predicted by the relationship  $0.86 \times SR_{0.64} - 0.02$ . In (a), the colored dots indicate the corresponding  $NDVI_{SWIR}$ . In (b), the colored dots indicate the corresponding scattering angle. The correlation coefficients and RMSE are given at the top of each panel. The black solid lines and error bars represent the average values and standard deviations for each bin.

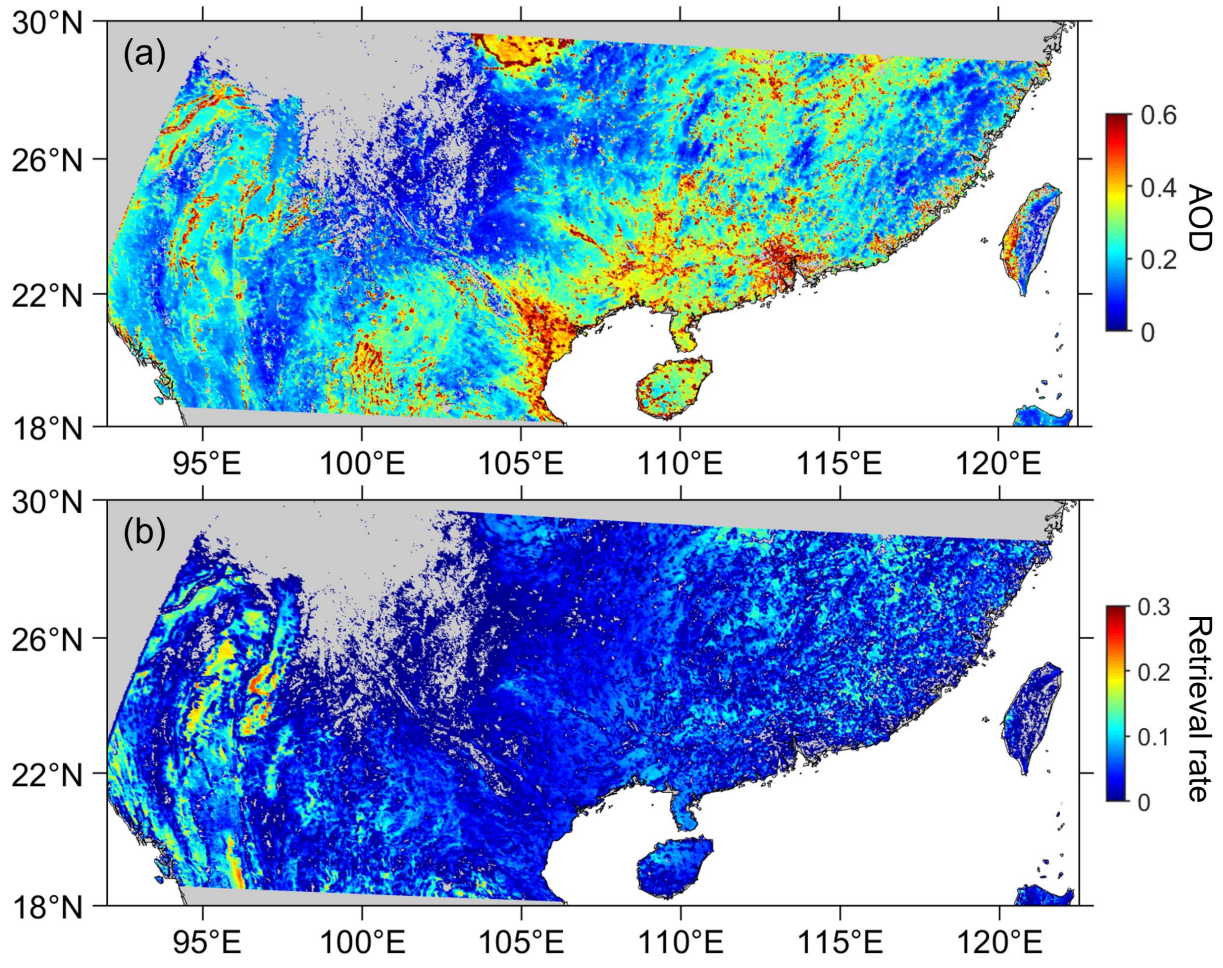


**Fig. S2.** Spatial distributions of (a) mean AOD and (b) available retrieval rate derived from DTDL. High-quality AOD retrievals are used here.

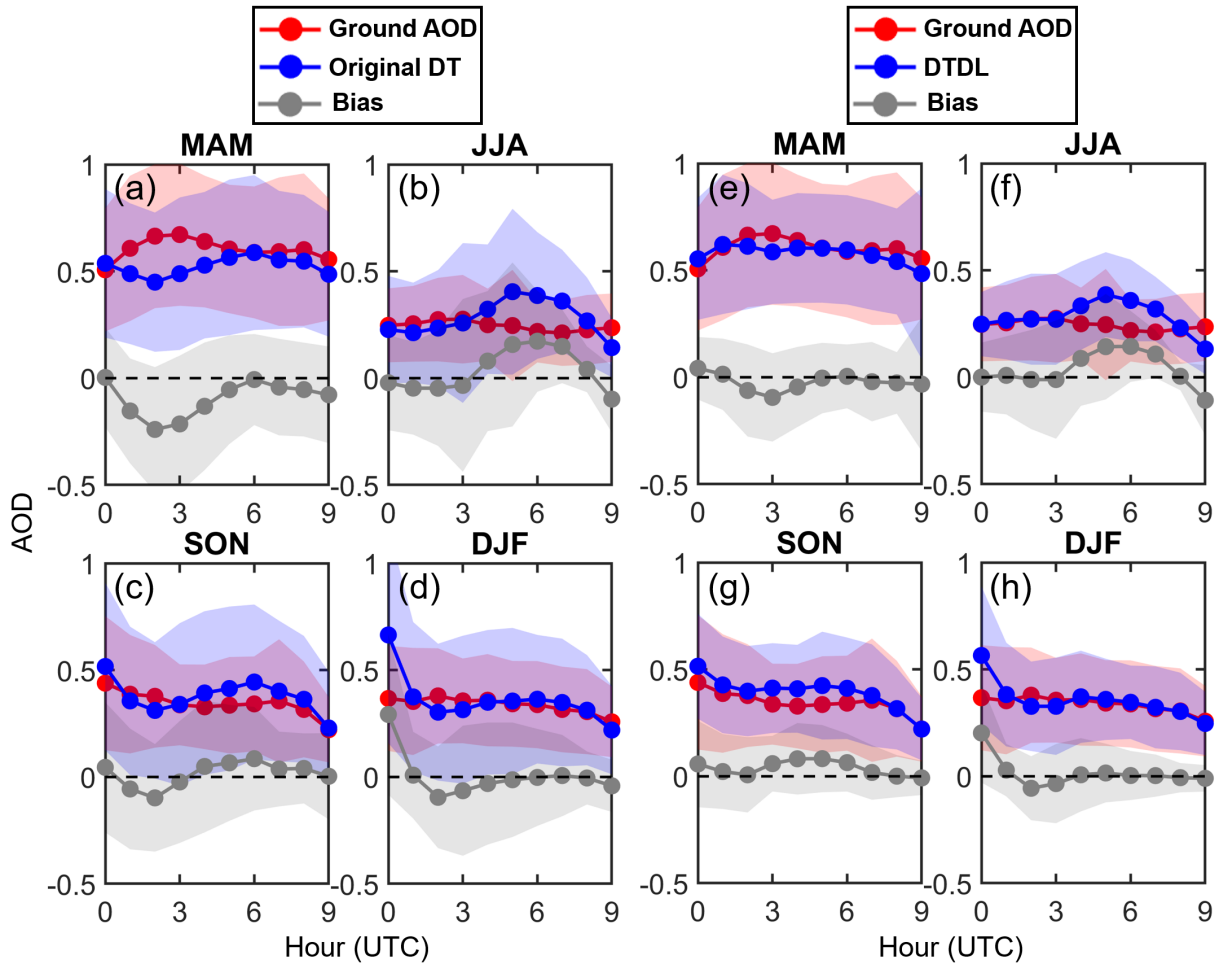


**Fig. S3.** Diurnal variation of Himawari-8/AHI AOD retrievals derived from (a-d) the original DT and (e-h) DTDL for different seasons (i.e. MAM, JJA, SON, and DJF). Here, all matched pairs of AHI retrievals and ground measurements are used. The diurnal variation derived from ground-based measurements is shown in red, and the bias between AHI and ground AOD is shown in grey. The shaded areas represent the standard deviations.

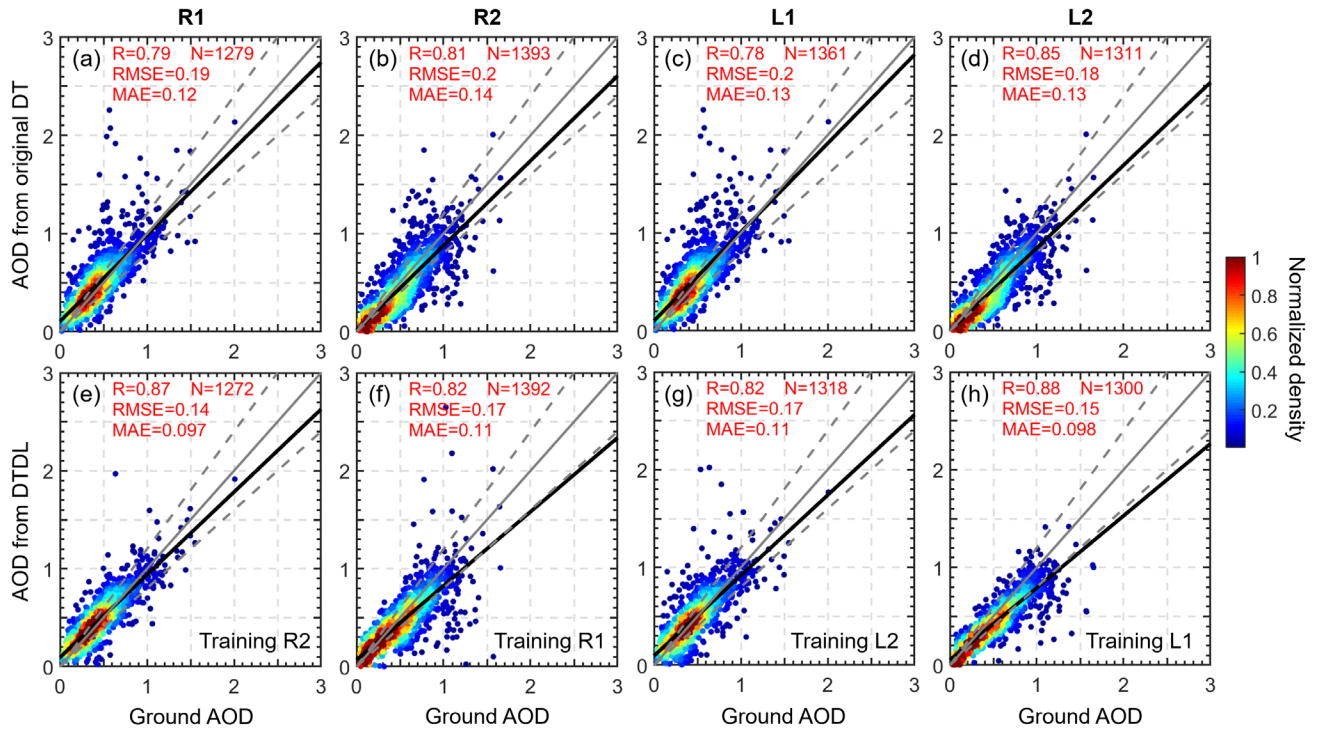


**Fig. S4.** Comparisons between ground AOD and AOD derived from original DT method over regions of (a) R1, (b) R2, (c) L1, (d) L2. Comparisons between ground AOD and AOD derived from DTDL over regions of (e) R1, (f) R2, (g) L1, (h) L2, while the training datasets are obtained over the regions of (e) R2, (f) R1, (g) L2, (h) L1 respectively. This process ensures independence of the validation dataset. The correlation coefficients, RMSE, sampling numbers, and MAE are given in each panel. High-quality AOD retrievals are used here.

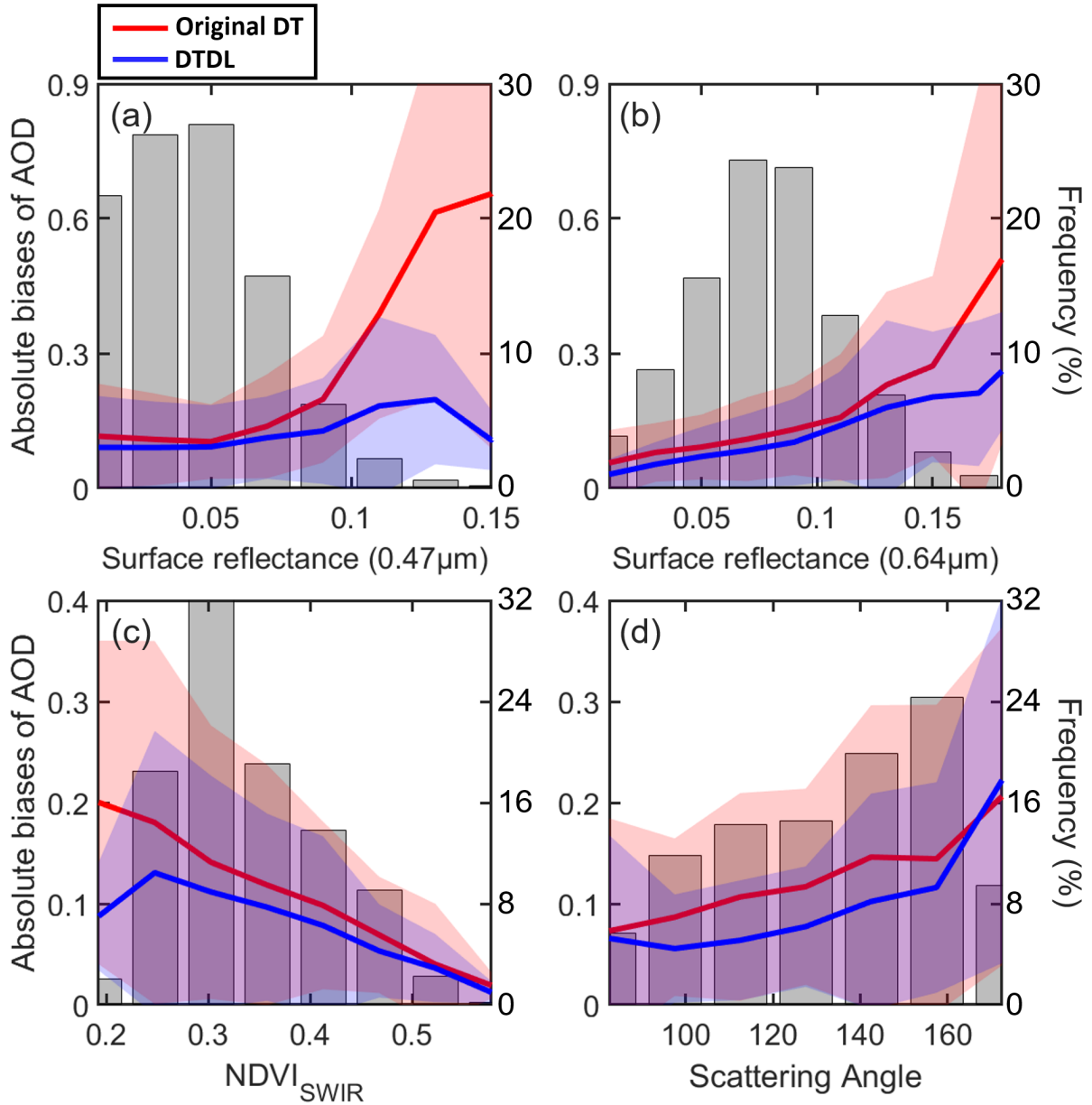


**Fig. S5.** Absolute biases between AOD derived from ground AOD and AHI, for different (a)  $SR_{0.47}$ , (b)  $SR_{0.64}$ , (c)  $\text{NDVI}_{\text{SWIR}}$ , and (d) Scattering Angle. Original DT (red lines) and DTDL (blue lines) are used respectively. The shaded areas indicate the standard deviations. The grey bars represent the frequency of occurrence for these parameters. High-quality AOD retrievals are used here.

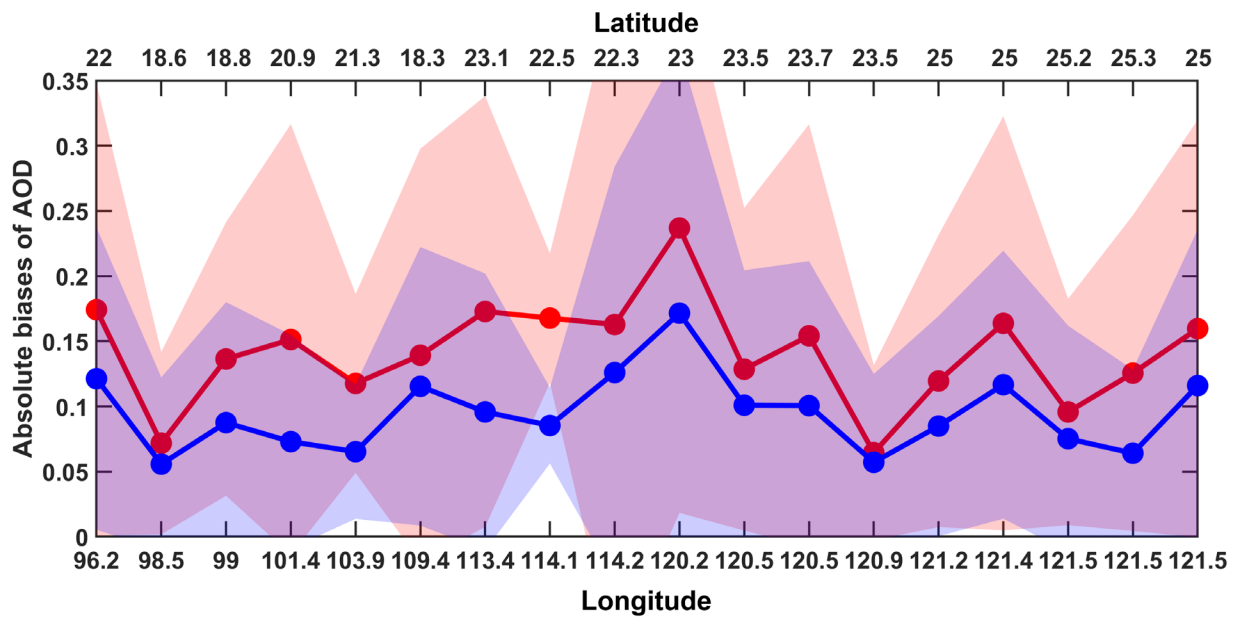


**Fig. S6.** Absolute biases between AOD derived from ground AOD and AHI at 18 sites. The original DT (red lines) and DTDL (blue lines) are used, respectively. The latitude and longitude for each site are marked in the x-axis. The shaded areas indicate the standard deviations.